PIAS1-FAK Interaction Promotes the Survival and Progression of Non-Small Cell Lung Cancer

CrossMark

Jerfiz D. Constanzo*, Ke-jing Tang*,†, Smita Rindhe*, Margherita Melegari*, Hui Liu‡, Ximing Tang‡, Jaime Rodriguez-Canales‡, Ignacio Wistuba‡,§ and Pier Paolo Scaglioni*

*Department of Internal Medicine and Simmons Comprehensive Cancer Center, University of Texas Southwestern Medical Center Dallas, TX, USA; †Department of Pulmonary Medicine, The First Affiliated Hospital of Sun Yat-sen University, Guangzhou, Guangdong, China; ‡Department of Translational Molecular Pathology, Head & Neck Medical Oncology, The University of Texas MD Anderson Cancer Center, Houston, TX, USA; §Department of Thoracic, Head & Neck Medical Oncology, The University of Texas MD Anderson Cancer Center, Houston, TX, USA

Abstract

The sequence of genomic alterations acquired by cancer cells during tumor progression and metastasis is poorly understood. Focal adhesion kinase (FAK) is a non-receptor tyrosine kinase that integrates cytoskeleton remodeling, mitogenic signaling and cell survival. FAK has previously been reported to undergo nuclear localization during cell migration, cell differentiation and apoptosis. However, the mechanism behind FAK nuclear accumulation and its contribution to tumor progression has remained elusive. We report that amplification of *FAK* and the SUMO E3 ligase *PIAS1* gene loci frequently co-occur in non-small cell lung cancer (NSCLC) cells, and that both gene products are enriched in a subset of primary NSCLCs. We demonstrate that endogenous FAK and PIAS1 proteins interact in the cytoplasm and the cell nucleus of NSCLC cells. Ectopic expression of *PIAS1* promotes proteolytic cleavage of the FAK C-terminus, focal adhesion maturation and FAK nuclear localization. Silencing of *PIAS1* deregulates focal adhesion turnover, increases susceptibility to apoptosis *in vitro* and impairs tumor xenograft formation *in vivo*. Nuclear FAK in turn stimulates gene transcription favoring DNA repair, cell metabolism and cytoskeleton regulation. Consistently, ablation of *FAK* by CRISPR/Cas9 editing, results in basal DNA damage, susceptibility to ionizing radiation and impaired oxidative phosphorylation. Our findings provide insight into a mechanism regulating FAK cytoplasm-nuclear distribution and demonstrate that FAK activity in the nucleus promotes NSCLC survival and progression by increasing cell-ECM interaction and DNA repair regulation.

Introduction

Protein inhibitor of activated STAT1 (*PIAS1*) is a SUMO E3 ligase implicated in the regulation of several oncogenes and tumor suppressors such as AKT, BRCA1, BRCA2, PML and PML-RARA [1–4]. In addition, *PIAS1* is over-expressed in prostate and lung cancers [4,5]. Moreover, increase in PIAS1 protein levels has recently been linked to breast cancer tumorigenesis, albeit reports disagree as to the relevance of

PIAS1 to tumorigenesis and metastasis [6,7]. Thus, we decided to characterize the relevance of PIAS1 in non-small cell lung cancer (NSCLC) progression and metastasis. We also investigated PIAS1 downstream targets that could account for the phenotype observed and potentially serve as a therapeutic target in NSCLC.

Lung cancer metastasis is an indicator of poor prognosis and a main determinant of cancer-related mortality. Consequently, targeting and prevention of cancer cell metastasis is among the biggest hurdles in clinical oncology [8]. During metastasis, cancer cells rely heavily on cell-extracellular matrix (ECM) interactions, cytoskeleton remodeling and gene transcription. An important player in these processes is focal adhesion kinase (FAK). FAK is a non-receptor tyrosine kinase that contributes to almost every aspect of metastasis; from ECM sensing, cytoskeleton remodeling to gene transcription [9–12]. The *FAK* gene is rarely mutated in human lung cancers, but the *FAK* locus (chromosome 8q) is frequently amplified in lung, colon, breast and gastric tumors [13–16].

FAK controls cytoskeleton remodeling by transducing signals from integrin receptors to ERK/MAPK, PI3K, RAC1 and RHOA [10,17–19]. Importantly, FAK promotes integrin β1 (ITGβ1) gene expression, which in turn, increases the survival of cancer cells [20]. FAK has also been linked to transcriptional activation of *SNAIL*, *TWIST*, *ZEB1*, and *ZEB2* genes, which are essential for epithelial to mesenchymal (EMT) reprogramming in epithelial cells [21–23]. However, whether FAK is involved in transcriptional regulation is still a matter of debate because FAK resides mainly in the cytoplasm where it is associated with the plasma membrane. However, FAK protein can relocate to the cell nucleus during cell differentiation or cancer progression [24,25]. Despite several studies reporting FAK protein nuclear localization and involvement in gene transcription, no unifying mechanism exists to explain the nuclear accumulation of FAK and the potential implications of nuclear FAK for tumorigenesis and metastasis.

Small ubiquitin-like modifiers (SUMO) have recently gained attention because of their participation in the covalent modification of target protein substrates, a process referred to as SUMOylation. This process consists of an enzymatic cascade whereby SUMO proteins are added onto target substrates with the involvement of E1, E2 and a limited number of SUMO E3 ligases. Typically, only a small fraction of a given protein is SUMOylated [26]. SUMOylation has been implicated in several cellular processes that include the regulation of nuclear import, DNA damage repair and signal transduction, however its role in tumorigenesis is still incompletely understood [27].

Using single nucleotide polymorphism (SNPs) data, we discovered that *PIAS1* and *FAK* are frequently co-amplified in lung cancer specimens. We found a positive correlation between increased gene copy number and FAK and PIAS1 protein levels in a subset of NSCLC cell lines *in vitro*, human lung tumor samples *in vivo* and in a mouse model of tumor metastasis. Herein, we report an interaction between FAK-PIAS1 leads to FAK nuclear relocation, which is crucial for the regulation of the turnover of focal adhesions, and cell survival during oncogenic stress.

Materials and Methods

Gene Copy Number Analysis
SNP was performed as previously described [4]. Briefly, SNP profile was obtained using Illumina DNA analysis Bead Chip (Illumina, Inc.). *PIAS1* and *FAK* gene copy number was extrapolated from their relative probe intensity compared with diploid controls.

Histochemistry and Immunofluorescence
Formalin-fixed, paraffin-embedded NSCLC specimens were obtained from the human tumor tissue bank at UT Southwestern Medical Center. Tissues and cells were processed for immunohistochemistry (IHC) or immunofluorescence (IF) using standard protocols [19]. See also supplementary methods.

Cell Lines and Tissue Culture
Human NSCLC cells and human bronchoalveolar epithelial cells (HBECs) were from the Hamon Center Cell Line Repository and were a gift of Dr. John Minna (UT Southwestern Medical Center) [28,29]. All cell lines were DNA-fingerprinted for provenance (PowerPlex 1.2 Kit; Promega) and Mycoplasma-free (e-Myco Kit; Boca Scientific). NSCLC cells were cultured in RPMI supplemented with 5% serum and antibiotics. HBEC cells were grown in keratinocyte growth media with supplements (Invitrogen, No.: 17005-042). NIH 3T3 were grown in 5% DMEM. All cells were maintained in humidified incubator with 5% CO_2 at 37°C. See also supplementary methods.

Western Blotting and Immunoprecipitation
We followed standard protocols [19].

Soft Agar Colony Formation, Transwell Migration and Scratch Assays
We performed these assays following established procedures [11,30].

Subcellular Fractionation
Cellular fractionation was carried out as previously described [31]. Cells were scraped with ice-cold PBS, pelleted by centrifugation at 600 g for 5 minutes, suspended in hypotonic lysis buffer (10 mM Tris-base pH 7.5, 10 mM KCl, 1.5 mM $MgCl_2$) with protease/phosphatase inhibitors for 10 minutes. Cells were then lysed by Dounce homogenization and centrifuged at $3000 \times g$ to separate cytoplasmic (supernatant) from nuclear (pellet) fractions. To extract nuclear proteins, the nuclear pellet was resuspended in high salt buffer (50 mM Tris-base, pH 7.9, 0.5 M NaCl) 2 mM EDTA, 10% sucrose, 10% glycerol) with protease and phosphatase inhibitors.

RNAi Interference
Stable lentiviral transduction was performed with pGIPZ Lentiviral vectors containing shRNAs targeting *PIAS1* and non-targeting scrambled shRNA controls (Dharmacon). siRNA (siGenome) targeting *PIAS1*, or non-targeting siRNA controls were purchased from Dharmacon. See also supplementary methods.

Oxygen Consumption Rate Measurement
This assay was performed with a Seahorse XF analyzer following the manufacturer's protocols (Seahorse Bioscience).

Mouse Xenografts
Xenografts were performed as described previously [32] and were approved by the institutional IACUC guidelines.

Results

FAK and PIAS1 Genes are Frequently Co-Amplified in a Subset of NSCLCs
Using SNPs gene copy number analysis we looked for novel genomic cooperating alterations in a panel of 108 non-small cell lung cancer (NSCLC) cells. This analysis revealed that approximately 8%
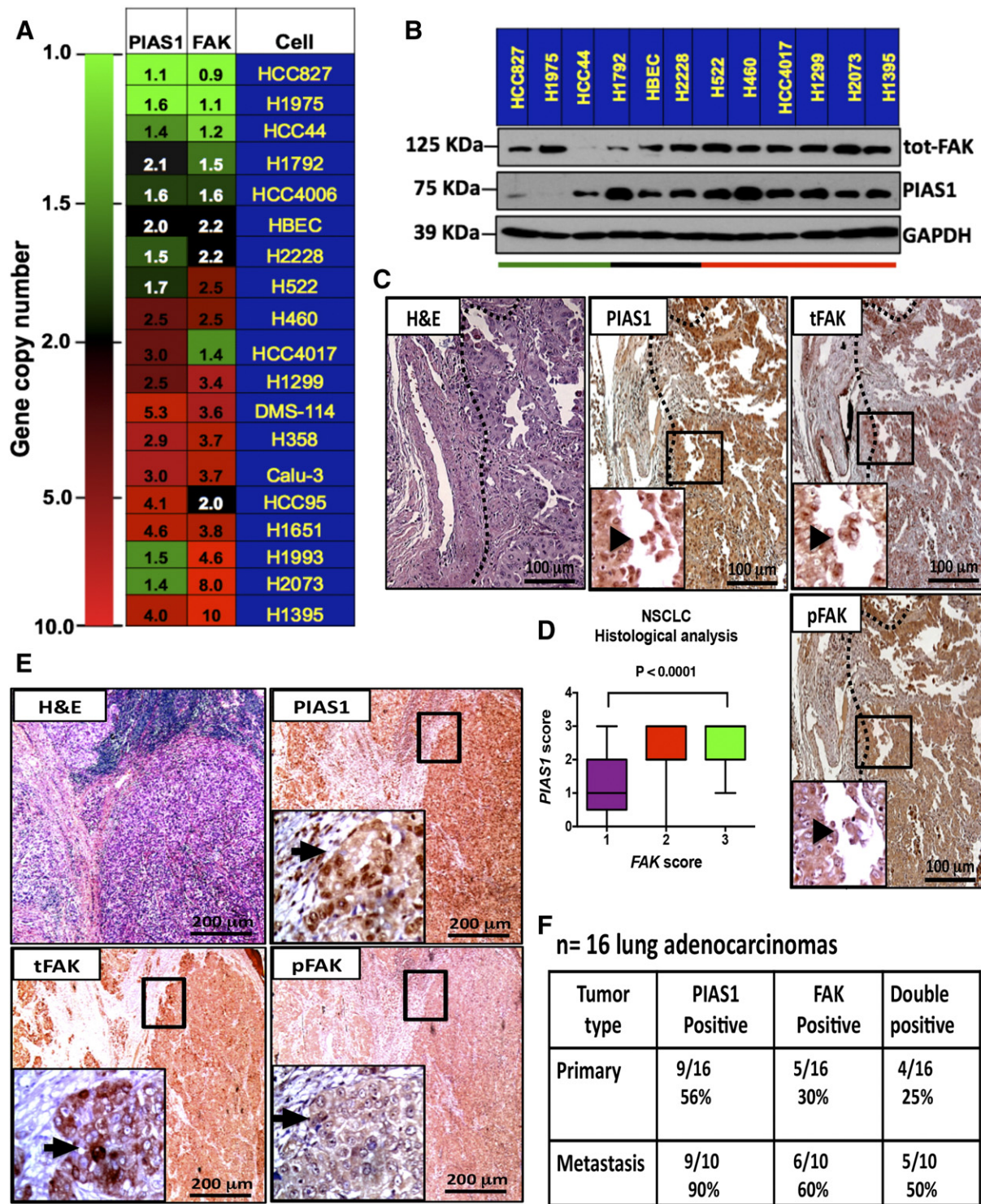
Figure 1. FAK and PIAS1 protein levels are correlated in NSCLC. (A) Heatmap shows single nucleotide polymorphism (SNPs) gene copy number analysis for *FAK* and *PIAS1* genes in the indicated lung cancer cell lines. Green, black and red indicate copy number loss, no change or gene copy number gain, respectively. (B) Immunoblot confirms increment in FAK and PIAS1 at the protein level in a representative panel of cells with gene amplification. Green, black and red horizontal lines indicate NSCLC cells with loss, no change or gene copy number gain of *PIAS1* and *FAK*. (C) Hematoxylin and eosin (H&E) and IHC stain of PIAS1, phospho-FAK (pFAK) and total FAK in primary NSCLC samples. Insert shows cytoplasmic and nuclear positivity for both proteins (black arrowheads). Scale bar: 100 μm. (D) IHC positivity score analysis of FAK and PIAS1 in human NSCLC tumor tissue microarrays samples (n = 330). Graph shows positive correlation between increase positivity in FAK stain and PIAS1. Score = 1 low intensity; 2 = moderate intensity; 3 = high intensity. Statistical analysis was done using a Mann-Whitney U test. (E) H&E and IHC stain of PIAS1, phospho-FAK (pFAK) and total FAK in metastatic NSCLC. Insert shows positivity for cytoplasmic and nuclear stain for both proteins. Scale bar: 200 μm. (F) Contingency table shows positive correlation between FAK and PIAS1 IHC stain positivity in primary *vs* metastatic samples. The number of samples is indicated.

(ie, 12 cell lines) of NSCLC cells had amplification of the *FAK* and/or *PIAS1* genes (Figure 1*A*).

To investigate the relationship between gene copy number gain and gene expression we detected FAK and PIAS1 by immunoblot in cell lines representative of our larger panel of NSCLC cells. We found that cell lines with increased PIAS1 gene copy number display concordant increase in PIAS1 protein (Figure 1*B*). Since gene amplification/deletions may result from adaptive responses to selective pressures of tissue culture, we tested primary NSCLC specimens for FAK and PIAS1 proteins using IHC. We found that primary NSCLC samples exhibited elevated total FAK (tot-FAK), phospho-FAK (p-FAK; Y397) and PIAS1 positivity compared to normal surrounding tissue (Figure 1*C*, arrowhead). Using lung tumor tissue microarrays we further confirmed that samples with high tot-FAK positivity score had a concomitant increase in PIAS1 positivity, but not p-FAK positivity (Figure 1*D*). Because FAK is associated with cell migration [9,33], we tested paired primary and metastatic NSCLC samples for FAK and PIAS1 protein levels. As observed in primary lung tumor samples, we found a positive correlation with FAK and PIAS1 protein levels in lymph node metastasis, but not with p-FAK protein levels (Figure 1, *E* and *F*). These observations suggest that PIAS1 and total-FAK protein levels correlate with tumor progression, independent of FAK phosphorylation.

The *Kras*^{G12D}/*p53*^{R172H} mouse model (KP hereafter) faithfully recapitulates aggressive human lung adenocarcinoma, developing advanced lung tumors that are highly metastatic [34,35]. Metastatic lung tumors in this mouse model have been fully characterized and show elevated expression of the *ZEB1* transcription factor and activation of Notch1 and Jagged2 signaling pathways, recapitulating the EMT profiles associated with human metastatic NSCLC [36,37]. As in human NSCLC, we found that KP lung tumors are positive for total-FAK and PIAS1, but not for p-FAK (Supplementary Fig. 1A). Next we took advantage of 393P and 344SQ lung cancer lines, which are a pair of lung cancer cell lines derived from a KP lung specimen. 393P cells, were derived from a primary lung tumor, are epithelial and have low metastatic potential; while 344SQ cells were derived from a metastatic KP lung tumor, are mesenchymal and are highly metastatic [34]. In this experimental system we found that PIAS1 is significantly up-regulated *in vivo* and metastatic cell line 344SQ (Supplementary Fig. 1B).

In view of these findings, we concluded that co-amplification of *FAK* and *PIAS1* genes occurs in a subset of primary human NSCLC samples. Moreover, subsets of primary and metastatic NSCLC samples have elevated PIAS1 and tot-FAK protein levels.

PIAS1 and FAK Proteins Physically Interact in NSCLC

We tested whether FAK and PIAS1 physically interact with co-IP assays using NIH-3T3 cells transiently transfected with *FAK or PIAS1* cDNAs. We successfully co-immunoprecipitated FAK with PIAS1 from transfected NIH-3T3 cells (Figure 2*A*). Furthermore, we co-immuno-precipitated endogenous FAK and PIAS1 proteins in several NSCLC cells, which co-amplify *FAK* and *PIAS1* genes (Figure 2*B*).

To gain insights into the location and stimulus required for FAK and PIAS1 interaction, we performed cellular co-fractionation of endogenous proteins during serum starvation, apoptosis or mitogenic stimulation. To our surprise, we discovered that FAK and PIAS1 mostly co-purified in the cytosolic fractions, when cells were treated with protein kinase C inhibitor (PKCi: Calphostin-C, a proapoptotic agent), or serum for 2-4 hours post starvation, but not after stimulation with epithelial growth factor (EGF) (Figure 2*C* lanes 5, 7 and 10). Using IF and confocal microscopy we found significant co-localization of

endogenous FAK and PIAS1 at the nuclear periphery of serum treated cells (Figure 2*D*). We subsequently performed immunoblot and confocal co-localization studies with well-characterized organelle markers following serum stimulation. Although partial localization of PIAS1 and FAK can be seen with the endoplasmic reticulum protein Calnexin, the dominant sites of interaction contain the RAB11 and LAMP1, endosome associated proteins. These findings suggest that internalization of growth factor receptors complexes promote the association of FAK and PIAS1 proteins in endosomes localized in the cytoplasm and nuclear periphery (Supplementary Fig. 2A-C).

To begin testing the biological significance of the interaction between FAK and PIAS1, we determined the effects of *Flag-Pias1* and or SUMO overexpression on FAK proteins. We found that overexpression of *Flag-Pias1* or SUMO-1 did not promote a significant change in tot-FAK or p-FAK (Figure 2*E*). However, expression of *Flag-Pias1* or the combination of *Flag-Pias1* and SUMO1 resulted in the appearance of a lower molecular weight species of FAK (Figure 2*E* arrowheads).

FAK was previously reported to undergo proteolytic cleavage by Calpain proteases on its C-terminus to allow disengagement from focal adhesions [38]. To test whether PIAS1 contributes to FAK C-terminal cleavage we used a mutant (*Fak*^{V744G}) that abolishes FAK protein C-terminal cleavage. Indeed, we found that the *Fak*^{V744G} is resistant to PIAS1-induced FAK C-terminal proteolysis (Figure 2*F*).

Thus, we concluded that mitogenic signaling promotes FAK and PIAS1 physical interaction, which correlates with PIAS1-induced FAK C-terminal cleavage. Importantly, this phenotype is rescued by using a *FAK* mutant resistant to proteolytic cleavage.

PIAS1-FAK Interaction Regulates Focal Adhesion Dynamics

Endogenous PIAS1 is mostly nuclear, but can also be found scattered in the cytoplasm of lung cancer cells *in vivo* and *in vitro* (Figures 1*C* and 2*D*). We hypothesized that PIAS1-FAK interaction may affect focal adhesion dynamics and how cells integrate extracellular signaling. To test this hypothesis, we used RNAi to determine how *PIAS1* affects F-Actin stress fiber formation. We found that *PIAS1* silencing in lung cancer cells destabilizes F-Actin fibers and reduces Vinculin (VCL) localization to focal adhesions (Figure 3*A*). Then we tested if the opposite was true using HBECs, which are immortalized, but not transformed, by transduction of CDK4 and human Telomerase Reverse Transcriptase (hTERT) [29]. Indeed, we found that ectopic expression of *PIAS1* (*Flag-Pias1*) in HBECs increases VCL puncta at focal adhesions, while also promoting the nuclear localization of GFP-FAK (*GFP-Fak*) (Figure 3*B*). We further tested for changes in VCL puncta formation in live cells using mCherry labeled VCL (*mCherry-VCL*). We measured the formation, duration and turnover of mCherry-VCL focal adhesion, as inverse correlation to FAK-dependent turnover of focal adhesions [11,38]. Compared to control shRNA, *PIAS1* silencing increased the turnover of mCherry-VCL puncta; along the leading and lagging edge of cells (Figure 3, *C–F*). Furthermore, we found that *Flag-Pias1* gene expression induces membrane ruffle formation in fibroblasts and rescues endogenous VCL puncta loss in *GFP-Fak* overexpressing cells (Supplementary Fig. 3A, B). Finally, induction of membrane ruffles by PIAS1 correlates with increases in Rac1-GTPase and ROCK-1 protein levels without an increase in pFAK levels (Supplementary Fig. 3C).

In view of these findings we concluded that PIAS1 regulates focal adhesion dynamics by promoting FAK nuclear localization and directional cell motility.
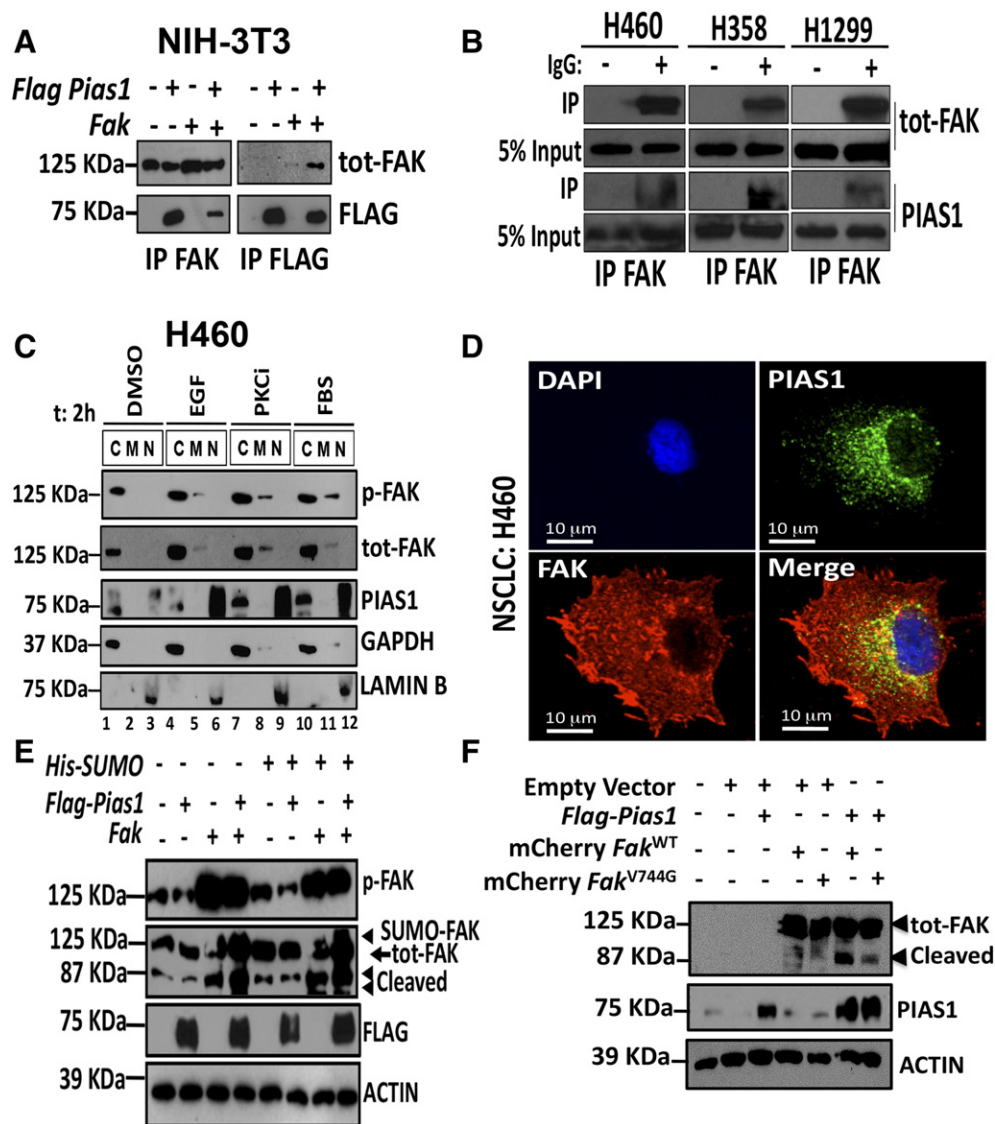
Figure 2. PIAS1 and FAK physically interact in human NSCLC cell lines. (A) NIH 3T3 cells were transiently transfected with the indicated plasmids and FAK and PIAS1 protein interaction was analyzed by co-IP followed by immunoblotting. (B) Immunoblot showing endogenous PIAS1 and FAK protein co-IP in the indicated NSCLC cell lines. (C) Subcellular fractionation and immunoblotting of endogenous FAK and PIAS1 proteins was performed in serum starved lung cancer cells H460 following treatment with: DMSO; EGF; protein kinase C inhibitor Calphostin (PKCi) and 10% FBS. Fractions: C; cytosolic; M; matrix; N: nuclear. Note significant cytoplasmic FAK and PIAS1 protein accumulation in PKCi and serum treatment, but not with EGF. (D) IF and confocal micrograph of FAK (red) and PIAS1 (green) localization at nuclear periphery in H460 NSCLC cells. Scale bar: 10um. (E) Immunoblot following *Flag-Pias1* and *Fak* overexpression in NIH-3T3. Blot shows no change in total FAK or pFAK (Y397), but note the appearance of low and higher molecular weight species of FAK protein in cells overexpressing *Flag-Pias1* or *Flag-Pias1-SUMO1* overexpression, which correspond to SUMOylated-FAK and cleaved FAK. (F) Cells were transfected with *mCherry-Fak^{wt}* or mCherry-*FAK^{V744G}*, a cleavage resistant mutation, in combination with *Flag*-Pias1 and analyzed with immunoblot as indicated. Note that *Flag-Pias1* promotes the cleavage of *mCherry-Fak^{wt}* as expected, but cleavage of C-terminus mutant *FAK^{V744G}* is impaired.
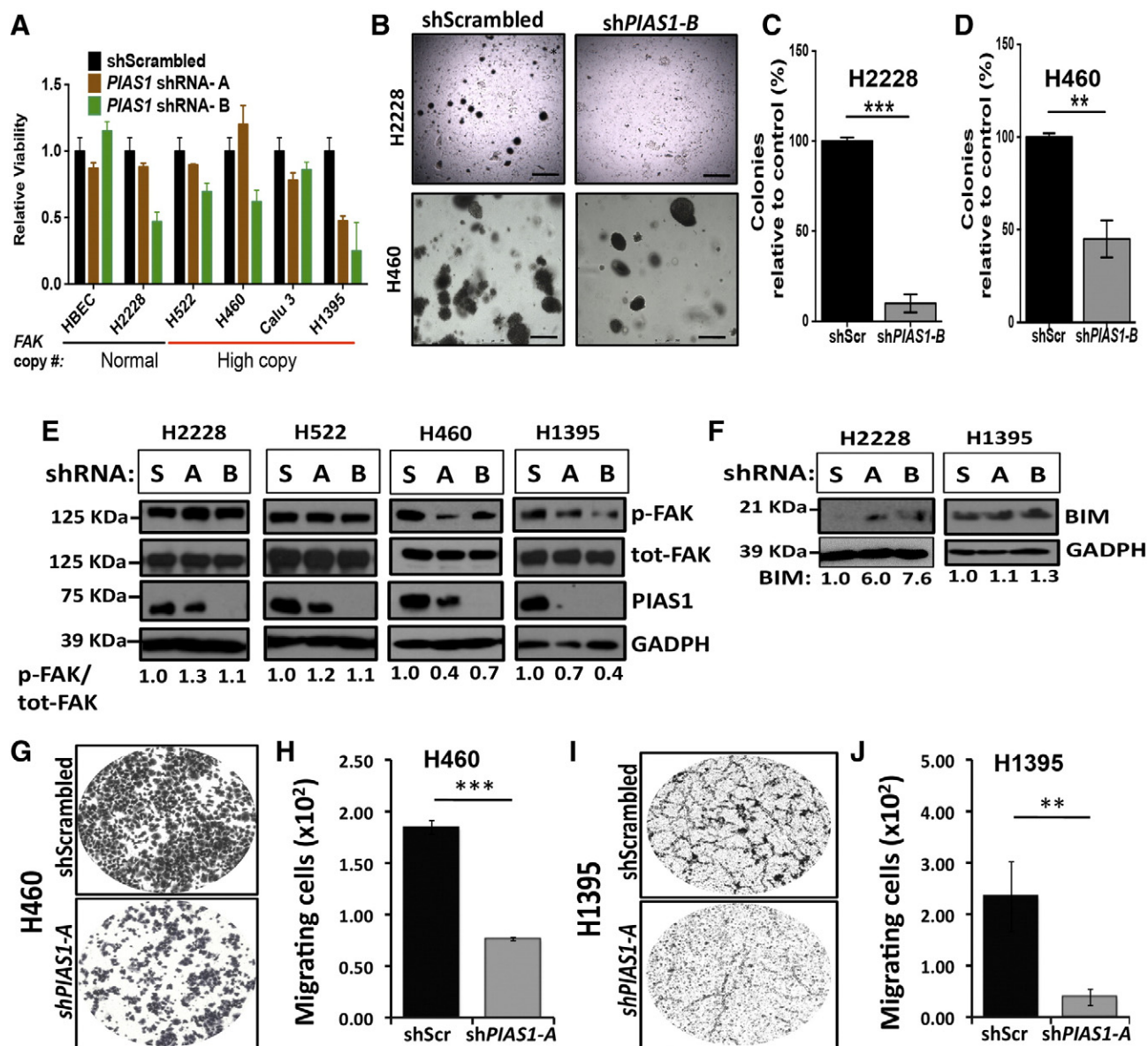
PIAS1 Silencing Impairs the Ability of NSCLC Cells to Form Colonies on Soft Agar

To elucidate how PIAS1-FAK interaction can modulate lung cancer progression we tested the effect of *PIAS1* inhibition on cell proliferation and survival. We found that *PIAS1* silencing with a short hairpin RNA (shRNA) had a modest effect on cell growth on plastic for most NSCLC cell lines (Figure 4A). Next, we examined how *PIAS1* inhibition would affect growth of NSCLC cells in soft agar. Indeed, following *PIAS1* inhibition, we observed a marked reduction in colony formation in soft agar assays (Figure 4, B–D).

Next we tested whether *PIAS1* inhibition may result in defective p-FAK activation, which could explain the inability of NSCLC cells with silenced *PIAS1* to establish colonies in soft agar assays. Surprisingly, p-FAK levels did not correlate with soft agar growth impairment in lung cancer cells (Figure 4E). Notably, the degree of knockdown achieved by shRNA A and B correlates with their effect on cell viability (Figure 4A). However, *PIAS1* silencing promotes increase baseline levels of pro-apoptotic protein BIM in several lung cancer cells including: H2228 and H1395 (Figure 4F). This finding suggests that *PIAS1* silencing does not directly affect p-FAK or
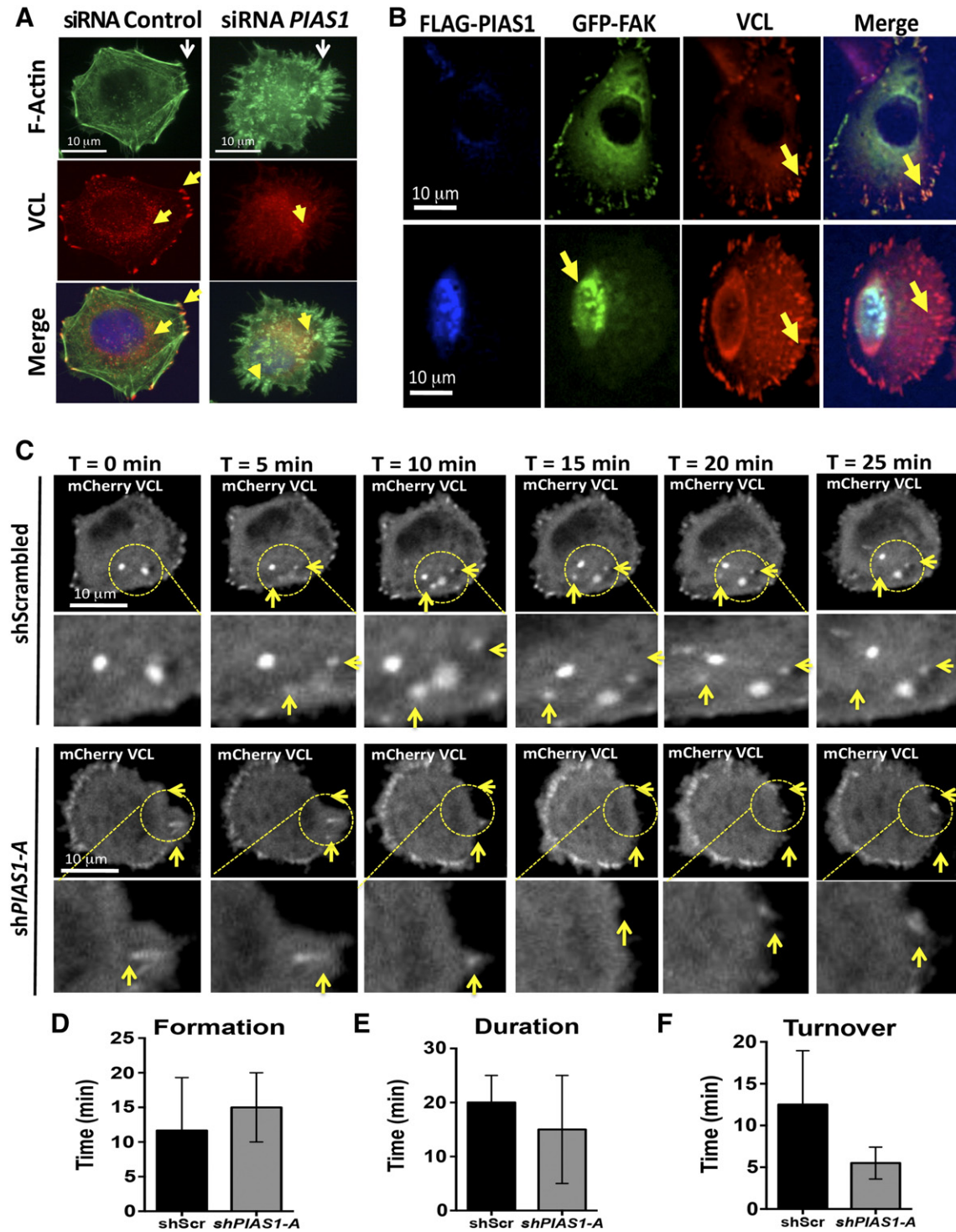
Figure 3. *PIAS1* silencing reduces stable stress fiber formation. (A) IF image of filamentous Actin (F-Actin) fiber formation in H460 NSCLC cells. White arrows indicate F-Actin fibers in control siRNA treated cells (Ctrl siRNA) or following *PIAS1* gene silencing; yellow arrows indicates Vinculin (VCL) protein localization to F-Actin fibers, which is lost in cells with *PIAS1* silencing. Scale bar: 10 μm. (B) IF image of VCL and GFP-FAK co-localization at F-Actin fibers in HBECs cells following ectopic *Flag-Pias1* expression. Top row shows HBECs cells expressing ectopic *GFP-Fak* and endogenous *VCL*. Bottom row image shows HBECs expressing ectopically expressed *Flag-Pias1* and GFP-FAK stained as indicated. Note FAK nuclear accumulation and increase in VCL puncta at focal adhesions (yellow arrows). Pink arrows indicate co-localization of GFP-FAK and VCL proteins. Scale bar: 10 μm. (C) Confocal live cell imaging of H460 NSCLC cells examining *mCherry-VCL* puncta formation dynamics in cells expressing the indicated shRNAs. Yellow arrows indicate sites of rapid focal adhesion turnover over a time lapse of 25 minutes. (D-F) Histograms show the average time for *mCherry-VCL* puncta formation, duration and turnover. Values represent an average of n = 3 cells.

Figure 4. *PIAS1* silencing impairs tumor progression in NSCLC cells with *FAK* gene amplification. (A) Histogram shows cell viability following *PIAS1* gene silencing. *FAK* gene copy number status is also indicated. (B) Representative soft agar colonies of NSCLC cells expressing the indicated shRNA. Scale bar: 500 μm. (C) Quantification of soft agar colonies of H2228 NSCLC cells 3 weeks post plating. (D) Quantification of soft agar colonies of H460 NSCLC cells 10 days post plating. (E) H2228, H522, H460 and H1395 NSCLC cells were treated with the indicated shRNAs and analyzed by Immunoblot with the indicated antibodies. (F) Immunoblot following *PIAS1* shRNA knockdown in H2228, H460 and H1395 NSCLC cells shows BIM pro-apoptotic protein upregulation. (G) Representative image of a Transwell migration assay performed with H460 cells expressing the indicated shRNAs. (H) Histogram shows the absolute number of migrating cells in triplicate wells following PIAS1 knockdown in lung cancer cell line H460. Student's *t* test = ***$P < .001$. (I) Representative image of a Transwell migration assay performed with H1395 cells expressing the indicated shRNAs. (J) Histogram shows the absolute number of migrating cells in triplicate wells following *PIAS1* knockdown in H1395 cells. Student's *t* test = **$P < .01$.

total-FAK protein levels in NSCLC, but promotes changes in FAK subcellular localization that are independent on FAK phosphorylation. Furthermore, these findings indicate that *PIAS1* silencing lowers the threshold for apoptosis in NSCLC cells.

Our analysis of human NSCLC samples suggested that PIAS1 and FAK proteins are elevated in a subset of highly invasive tumors. Thus, we tested whether *PIAS1* silencing affects NSCLC cell invasion and migration potential *in vitro*. To do this, we performed Transwell migration and scratch assays in NSCLC cells with gene amplification of *FAK* and *PIAS1* [21,30,39]. In Transwell assays, H460 cells expressing the control shRNA completed migration after 16 hours (16 h) [40],

whereas cells expressing a shRNA targeting *PIAS1* showed reduced migration through Transwell membranes (Figure 4, *G–H*). These findings were replicated in H1395 cells, another NSCLC cell line with gene amplification of *FAK* and *PIAS1* (Figure 4, *I–J*).

These results suggest that *PIAS*1 suppression significantly reduce the migration capacity of NSCLC cells. Thus, we performed scratch migration assays using NSCLC cells: H1792, H522 and H460 as representative examples of NSCLC cells from our panel. We found that *PIAS1* suppression did not have an effect on H1972, which has a loss of *FAK* gene copy number, but reduced the migration of H522 and H460, which have substantially higher levels of FAK and PIAS1

protein (Supplementary Figure 4, *A–F*). We assessed for changes in the cytoskeleton following scratch formation in H460 cells by staining for F-Actin and cells polarity with the GM130 Golgi maker. After 8 hours, cells transfected with the siRNA control were oriented towards the scratch site, whereas cells with *PIAS1* silencing were not, suggesting reduced ability to polarize towards the scratch site (Supplementary Figure 4, *G–H*).

In view of our findings we conclude that *PIAS1* suppression is associated with reduced anchorage-independent growth. In addition, *PIAS1* silencing reduces cell polarization during stimulus-driven migration in NSCLC cells with *FAK* and *PIAS1* gene amplification.

PIAS1-FAK Interaction Regulates Gene Transcription

We determined that *PIAS1* promotes focal adhesion maturation and FAK protein nuclear accumulation. This phenotype was conserved in NSCLC cells, NIH-3T3 fibroblasts and HBECs (Figure 5, *A–B*). GFP-FAK nuclear accumulation also occurs in HBECs cells harboring the oncogenic *KRAS*^{G12D} mutation and *p53* knockdown, suggesting a positive correlation with cancer progression (Figure 5B).

To test whether PIAS1-FAK interaction and FAK nuclear accumulation are directly associated with a pro-tumorigenic gene transcription program, we analyzed HBECs ectopically expressing *GFP-Fak and Flag-Pias1*. We analyzed mRNA-transcript linearized data with the Benjamini-Hochberg statistics (log ratio 0.6; and p value < 0.3) and subtracted values obtained from HBECs expressing *GFP-Fak* alone or *Flag-Pias1* alone to obtain transcripts that change only when both genes are co-expressed in HBECs. We identified 473 differentially up/down-regulated transcripts, which we used for further characterization (GEO accession ID: GSE73280). Using gene ontology analysis we uncovered that co-expression of *GFP-FAK* and *PIAS1* correlates with activation of several transcriptional programs that include DNA damage repair genes, oxidative phosphorylation genes and a pancreatic adenocarcinoma signature (Figure 5D). This finding suggests that nuclear FAK may participate in DNA repair and cell cycle progression, a hypothesis consistent with the known function of PIAS1 in these processes [1,5].

To test whether *FAK* is involved in DNA repair or mitochondrial metabolism, we targeted its deletion in NSCLC cells by CRISPR/Cas9 gene editing. First, we tested for changes in γH2AX and pCHK2, which are well-known DNA damage response genes [31,41]. We found that in addition to having baseline activation of γH2AX and phospho-Chk2 (pCHK2), surrogate markers of DNA damage, *FAK* null (*FAK*⁻) H460 NSCLC cells were hypersensitive to ionizing radiation (IR) (Figure 5E). This result suggests a link between FAK nuclear localization and DNA damage response in NSCLC cells. We also tested the effect of *FAK* loss on oxidative phosphorylation by assessing ATP production and oxygen consumption rate. We found that in agreement with the perturbation in oxidative phosphorylation signatures during PIAS1-FAK overexpression, FAK protein depletion by CRISPR/Cas9 led to a reduced mitochondria ATP production and oxygen consumption rates (Figure 5, *F* and *G*).

Taken together these results suggest that PIAS1, by promoting FAK nuclear localization, promotes tumor progression by engaging transcriptional programs that regulate DNA damage repair, and oxidative phosphorylation.

PIAS1 Silencing is Detrimental for Xenograft Tumor Growth In Vivo.

Lastly, we examined whether *PIAS1* was required for tumor engraftment *in vivo* by performing xenograft experiments. We compared

H460 cells growth rate *in vivo* following stable viral transduction of control shRNA or a *PIAS1* shRNA. Xenografts expressing *PIAS1* shRNA showed a significant reduction in growth 15 days post implantation as compared to controls (*P* < .05) (Figure 6A). Furthermore, mice in the control group were euthanized on average after 37-days due to tumor burden; whereas the survival of mice in the PIAS1 shRNA group averaged 55 days (Figure 6B). We performed postmortem histological analysis of xenograft tumors and found no significant difference in cell morphology or vascularity (Figure 6C). We then examined the contribution of shRNA harboring cells to the xenograft using the GFP reporter in the shRNA vector backbone and discovered a significant underrepresentation of GFP positive cells in the *PIAS1-shRNA* treatment group as compared to shRNA controls (**P* < .05) (Figure 6, *D–E*).

In view of these findings, we concluded that *PIAS1* is required for the growth of tumor xenografts *in vivo*. Furthermore, *PIAS1* inhibition is selected against during tumor growth as demonstrated by the underrepresentation of *PIAS1* shRNA expressing cells at the experiment endpoint.

Discussion

Metastasis accounts for more than 90% of cancer related deaths worldwide [34,35,42,43]. Consequently, identification of novel biomarkers and potential therapeutic targets is of paramount importance. FAK nuclear localization has been reported to be important for disease progression in various cancer types and a requirement during embryogenesis and tissue homeostasis [40,44,45]. However, the mechanism that mediates FAK relocation to the cell nucleus and if and how this enhances cell survival, metastasis and tissue development has remained unclear [25,46].

Using SNPs data, we discovered that the SUMO-E3 ligase *PIAS1* and *FAK* genes are co-amplified in a subset of NSCLC specimens. Furthermore, we show a positive correlation between gene copy number gain and increase in total FAK and PIAS1 protein levels, using NSCLC cell lines *in vitro* and human lung tumor samples *in vivo*. Interestingly, we found that FAK and PIAS1 protein are elevated in a subset of primary and invasive human lung tissues and in a *bona fide* mouse model of NSCLC metastasis [35].

It was previously reported that FAK and PIAS1 protein interact in a yeast two-hybrid screen and in transfected HEK-293T cells. In this setting PIAS1 promotes FAK phosphorylation at tyrosine 397 (Y397), a key event for FAK activation [47]. We confirmed that endogenous PIAS1 and FAK interact in NSCLC cells and this interaction is observed at the nuclear periphery or within the cell nucleus. However, our findings indicate that *PIAS1* expression does not affect P-FAK or total FAK protein levels in NSCLC, instead our data support the conclusion that PIAS1 promotes changes in FAK subcellular localization that are independent on its phosphorylation. Indeed, *PIAS1* expression, or the combined expression of *PIAS1* and *SUMO-1*, results in the appearance of a ~87 KDa form of FAK, previously reported as a Calpain-mediated FAK cleavage product [38]. Indeed we found that using a point mutant form of FAK protein (*Fak*^{V744G}), that renders FAK resistant to Calpain proteolysis, the ~87KDa form of FAK was significantly reduced. Because FAK cleavage is part of its negative regulation at focal adhesions, we conclude that PIAS1 may be involved in the regulation of FAK and focal adhesion dynamics.

Recently, inhibition of *PIAS1* was found to reduce breast cancer tumorigenesis by increasing genomic instability and loss of stem cell potential [7]. Silencing of *PIAS1* in a subset of NSCLC cells with *FAK*
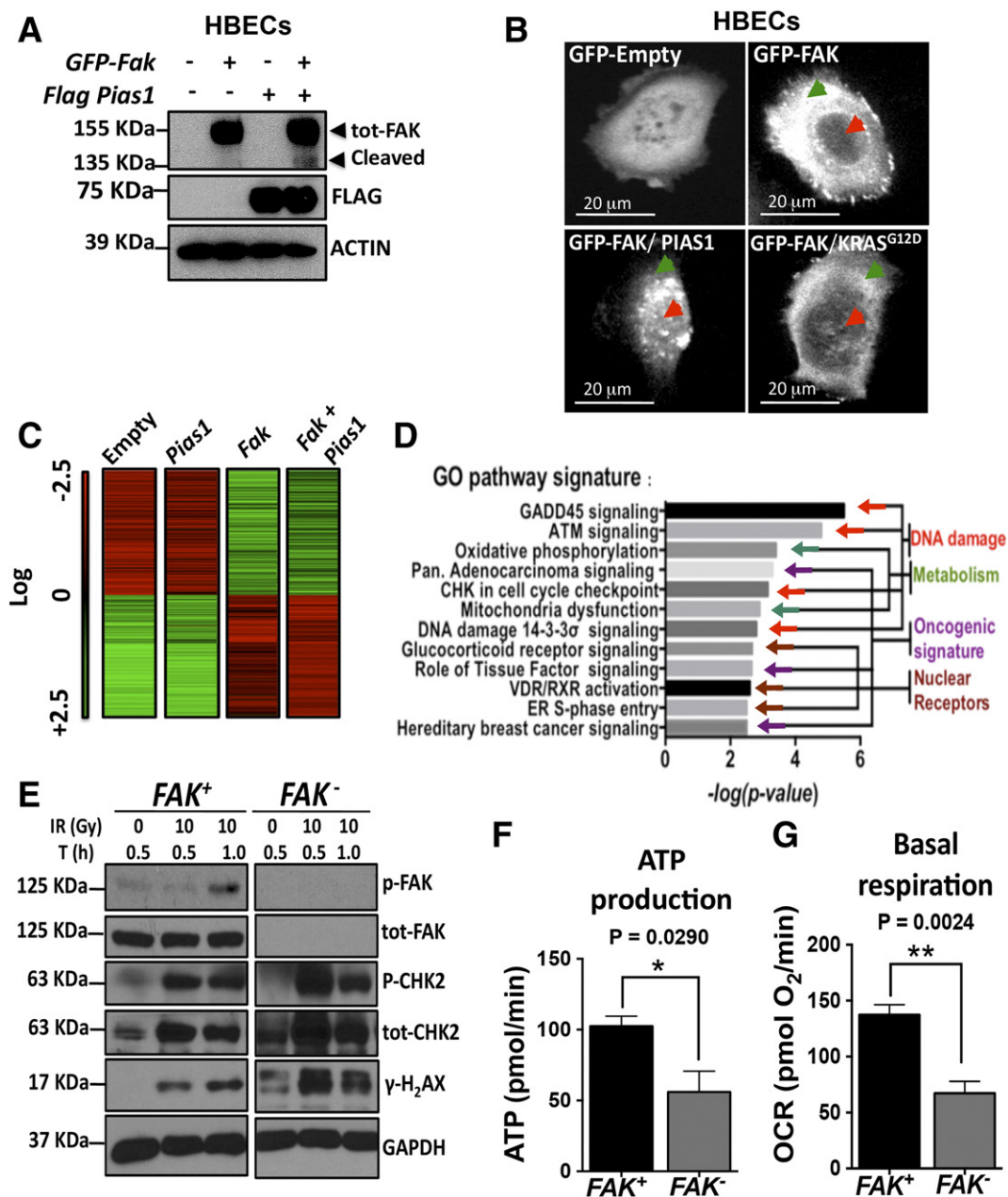
Figure 5. PIAS1 promotes FAK protein nuclear localization and gene transcription. (A) Immunoblot of immortalized HBECs transduced/transfected with the indicated plasmids. Arrow indicates cleaved FAK. (B) Confocal microscopy of HBECs transduced as indicated. Note the nuclear relocation of GFP-FAK after either ectopic *Flag-Pias1* overexpression in HBECs or cells harboring *KRAS*[G12D] mutations (green and red arrows indicate cytoplasmic and nuclear FAK, respectively). Scale bar: 20 μm. (C-D) Heatmap and gene ontology analysis of HBECs expressing *GFP-Fak* alone or in combination with *Flag-Pias1*. (E) Immunoblot of *FAK* wild type (*FAK*[+]) or *FAK* deleted (*FAK*[-]) H460 NSCLC cells treated with IR and harvested at the indicated time points. Note upregulation of p-CHK2 and g-H$_2$AX in null cells, indicating DNA damage hypersensitivity following *FAK* loss. (F) Histogram shows the change in ATP productions (pmol/min) and oxygen consumption rate (OCR) in H460 NSCLC following FAK gene deletion. Analysis of mitochondrial function shows reduced ATP production and oxygen consumption in *FAK*^{-} H460 cells.

amplification results in deregulated F-Actin formation and increase in focal adhesion turnover. We found that *PIAS1* expression can promote GFP-FAK nuclear accumulation and rescues the accumulation of VCL puncta at focal adhesions. The latter correlates with an increase in the activation of integrin downstream targets (RAC-1 and ROCK-1), but not pFAK activation, as it is no longer at the cell membrane where its phosphorylation is known to occur [48,49].

Although FAK is widely associated with metastasis [10,11,25], it is still unclear whether PIAS1 or SUMOylation negates or contributes

to tumor progression [5,50]. PIAS1 was reported to repress TGF-β and reduced EMT transition in breast cancer cells by repression of *N-cadherin* [6]. However, other reports suggest that PIAS1 is necessary for breast cancer progression via activation of WNT5A, regulation of the estrogen receptor (ER) signaling and promoting tumor growth *in vivo* [7]. In our study, we found that *PIAS1* silencing in NSCLC did not have an effect on EMT genes including *N-Cadherin or E-Cadherin* (JDC and PPS, unpublished data). However, *PIAS1* silencing in NSCLC reduced cell polarization and
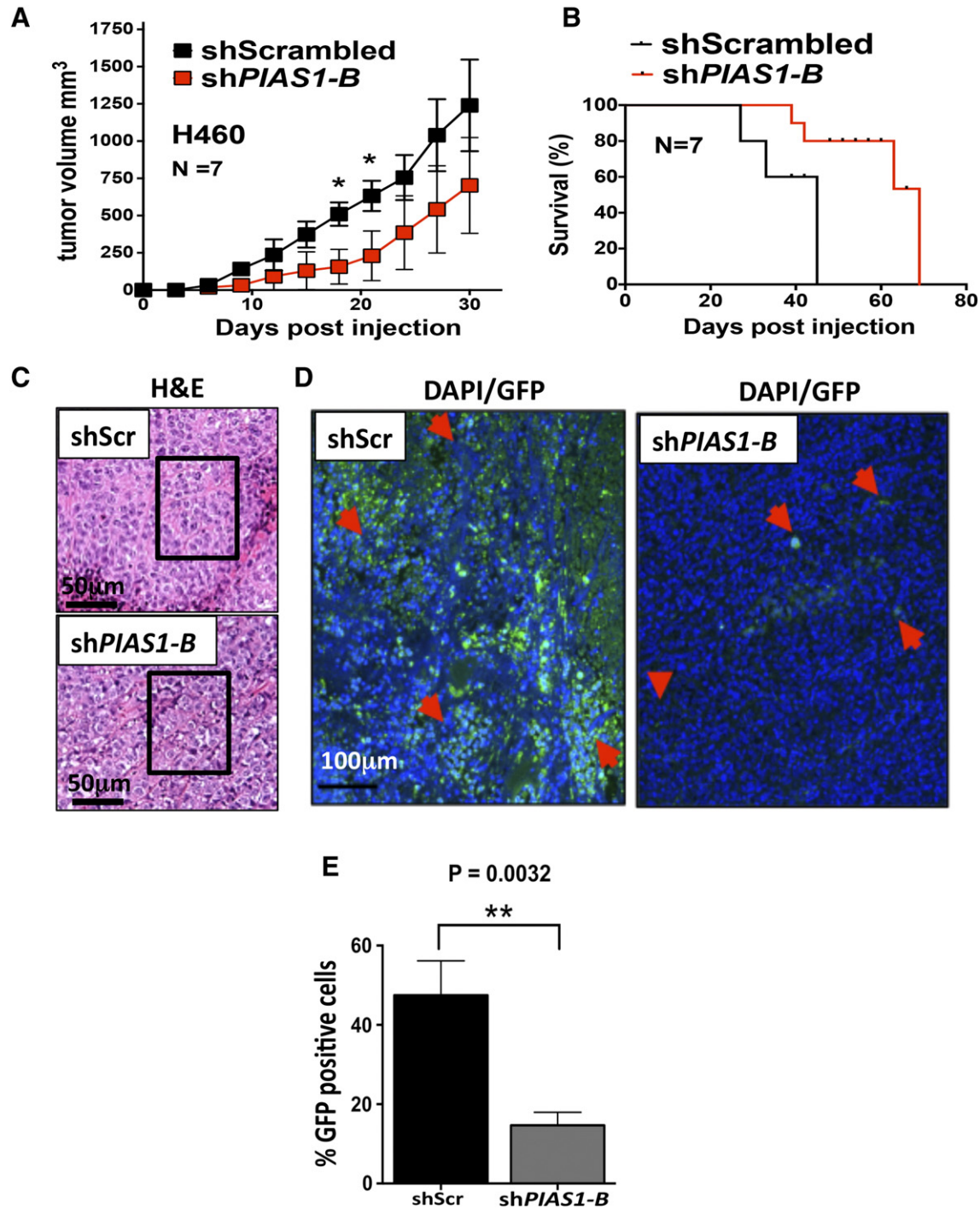
Figure 6. *PIAS1* gene silencing impairs xenograft tumor growth *in vivo*. (A) The histogram shows the volume of xenografts from H460 cells grown subcutaneously in NOD-SCID mice following transduction with scrambled shRNA (shScr; black line) or *PIAS1* shRNA (*shPIAS1*; red line). Mice per group N = 7. (B) Kaplan–Meier curve of mice carrying xenografts shown in panel A. Mice were sacrificed when the tumors reached 2000 mm^3. (C) H&E histological analysis of xenografts expressing shScr or *PIAS1* shRNA at the end point of the experiment. Squares indicate the sections analyzed for the GFP reporter in the shRNA construct. (D) Anti-GFP IF shows loss of GFP positive cells in the PIAS1 shRNA xenograft group compared to the scramble shRNA group. (E) Quantification of GFP positive cells in the indicated xenograft sections. Student's *t* test = **$P < .01$.

migration, suggesting that PIAS1 contributes to NSCLC stimulus-driven migration. Specifically, we observed deficient lamellipodia formation and GM130 leading edge orientation following migration stimulus *in vitro*, which may have contributed to cells inability to integrate extracellular signaling and properly migrate. We propose

that FAK recruitment to the nucleus by means of increase interaction with PIAS1, allows for focal adhesion maturation and increase integrin signaling, as demonstrated by the appearance of lamellipodia projections in *Flag-Pias1* expressing cells. In contrast, lamellipodia are decreased or absent in migrating cells after *PIAS1* knockdown. *PIAS1*

gene silencing in NSCLC cells also reduced cell viability, independently of P-FAK activation. Following *PIAS1* gene silencing we observed a concomitant increase in BIM protein levels. In addition, we also observed a significant decrease in soft agar growth following *PIAS1* knockdown.

An unexpected result in our study was that PIAS1-induced FAK nuclear recruitment promotes DNA repair transcription program. Because FAK deletion led to DNA-damage hypersensitivity, shown by γH2AX and pCHK2 activation, we speculate that the co-amplification of *FAK* and *PIAS1* promotes DNA damage repair, providing a survival advantage to genomically unstable tumors. In fact, FAK was found to be a negative regulator of p53 tumor suppressor in immortalized fibroblasts, and FAK inhibition radiozensitizes head and neck carcinoma [46,51]. Work is already in progress to characterize in better detail the involvement FAK in DNA damage repair and possible applications for NSCLC radiotherapy. Another unexpected finding was that silencing of *FAK* is associated with decrease of oxygen consumption and ATP production, an observation that underscores the importance of FAK in the maintenance of FAK-dependent NSCLC cells. Work is currently in progress to further characterize this phenotype.

In agreement with previous findings in breast cancer, *PIAS1* silencing affects NSCLC cells growth in soft agar *in vitro* and tumor xenograft growth *in vivo*. We speculate DNA damage regulation in NSCLC may provide the prosurvival signaling required for tumor progression in *PIAS1/FAK* overexpressing cancers. It will be of interest to identify the transcriptional modulators interacting with FAK while in the nucleus, as they represent potential tumor biomarkers or therapeutic targets.

Finally, our results show that a subset of NSCLCs has co-amplification of *FAK* and *PIAS1* and that these proteins are enriched in metastatic NSCLC. We conclude that PIAS1 is oncogenic and that, at least in part, this activity depends on its ability to promote FAK nuclear accumulation, integrin signaling activation and DNA damage repair. We conclude that the FAK-PIAS1 signaling axis is a novel regulator of NSCLC progression, integrating extracellular cues that regulate cell survival, migration and the DNA damage response. We propose that FAK-PIAS1 status would serve as a biomarker for the selection of patients undergoing personalized cancer treatment protocols likely to respond to FAK inhibitors currently in clinical trials.

Conflict of Interest
Authors declare no conflict of interest.

Author Contribution
JDC and PPS conceived the project, designed experiments and wrote the manuscript. JDC, KT, SM, HL and MM performed experiments; XT, JRC and IW performed and interpreted tumor microarray histochemistry experiments.

Acknowledgments

Appendix A. Supplementary data

References

[1] Galanty Y, Belotserkovskaya R, Coates J, Polo S, Miller KM, and Jackson SP (2009). Mammalian SUMO E3-ligases PIAS1 and PIAS4 promote responses to DNA double-strand breaks. *Nature* **462**, 935–939.

[2] Li R, Wei J, Jiang C, Liu D, Deng L, Zhang K, and Wang P (2013). Akt SUMOylation regulates cell proliferation and tumorigenesis. *Cancer Res* **73**, 5742–5753.

[3] Morris JR, Boutell C, Keppler M, Densham R, Weekes D, Alamshah A, Butler L, Galanty Y, Pangon L, and Kiuchi T, et al (2009). The SUMO modification pathway is involved in the BRCA1 response to genotoxic stress. *Nature* **462**, 886–890.

[4] Rabellino A, Carter B, Konstantinidou G, Wu SY, Rimessi A, Byers LA, Heymach JV, Girard L, Chiang CM, and Teruya-Feldstein J, et al (2012). The SUMO E3-ligase PIAS1 regulates the tumor suppressor PML and its oncogenic counterpart PML-RARA. *Cancer Res* **72**, 2275–2284.

[5] Hoefer J, Schafer G, Klocker H, Erb HH, Mills IG, Hengst L, Puhr M, and Culig Z (2012). PIAS1 is increased in human prostate cancer and enhances proliferation through inhibition of p21. *Am J Pathol* **180**, 2097–2107.

[6] Dadakhujaev S, Salazar-Arcila C, Netherton SJ, Chandhoke AS, Singla AK, Jirik FR, and Bonni S (2014). A novel role for the SUMO E3 ligase PIAS1 in cancer metastasis. *Oncoscience* **1**, 229–240.

[7] Liu B, Tahk S, Yee KM, Yang R, Yang Y, Mackie R, Hsu C, Chernishof V, O'Brien N, and Jin Y, et al (2014). PIAS1 regulates breast tumorigenesis through selective epigenetic gene silencing. *PLoS One* **9**, e89464.

[8] Frisch SM, Schaller M, and Cieply B (2013). Mechanisms that link the oncogenic epithelial-mesenchymal transition to suppression of anoikis. *J Cell Sci* **126**, 21–29.

[9] McKean DM, Sisbarro L, Ilic D, Kaplan-Alburquerque N, Nemenoff R, Weiser-Evans M, Kern MJ, and Jones PL (2003). FAK induces expression of Prx1 to promote tenascin-C-dependent fibroblast migration. *J Cell Biol* **161**, 393–402.

[10] Pylayeva Y, Gillen KM, Gerald W, Beggs HE, Reichardt LF, and Giancotti FG (2009). Ras- and PI3K-dependent breast tumorigenesis in mice and humans requires focal adhesion kinase signaling. *J Clin Invest* **119**, 252–266.

[11] Sieg DJ, Hauck CR, and Schlaepfer DD (1999). Required role of focal adhesion kinase (FAK) for integrin-stimulated cell migration. *J Cell Sci* **112**(Pt 16), 2677–2691.

[12] Wilson C, Nicholes K, Bustos D, Lin E, Song Q, Stephan JP, Kirkpatrick DS, and Settleman J (2014). Overcoming EMT-associated resistance to anti-cancer drugs via Src/FAK pathway inhibition. *Oncotarget* **5**, 7328–7341.

[13] Agochiya M, Brunton VG, Owens DW, Parkinson EK, Paraskeva C, Keith WN, and Frame MC (1999). Increased dosage and amplification of the focal adhesion kinase gene in human cancer cells. *Oncogene* **18**, 5646–5653.

[14] Golubovskaya VM, Conway-Dorsey K, Edmiston SN, Tse CK, Lark AA, Livasy CA, Moore D, Millikan RC, and Cance WG (2009). FAK overexpression and p53 mutations are highly correlated in human breast cancer. *Int J Cancer* **125**, 1735–1738.

[15] Park JH, Lee BL, Yoon J, Kim J, Kim MA, Yang HK, and Kim WH (2010). Focal adhesion kinase (FAK) gene amplification and its clinical implications in gastric cancer. *Hum Pathol* **41**, 1664–1673.

[16] Rodenhuis S, Slebos RJ, Boot AJ, Evers SG, Mooi WJ, Wagenaar SS, van Bodegom PC, and Bos JL (1988). Incidence and possible clinical significance of K-ras oncogene activation in adenocarcinoma of the human lung. *Cancer Res* **48**, 5738–5741.

[17] Carr HS, Zuo Y, Oh W, and Frost JA (2013). Regulation of focal adhesion kinase activation, breast cancer cell motility, and amoeboid invasion by the RhoA guanine nucleotide exchange factor Net1. *Mol Cell Biol* **33**, 2773–2786.

[18] Chang F, Lemmon CA, Park D, and Romer LH (2007). FAK potentiates Rac1 activation and localization to matrix adhesion sites: a role for betaPIX. *Mol Biol Cell* **18**, 253–264.

[19] Konstantinidou G, Ramadori G, Torti F, Kangasniemi K, Ramirez RE, Cai Y, Behrens C, Dellinger MT, Brekken RA, and Wistuba II, et al (2013). RHOA-FAK is a required signaling axis for the maintenance of KRAS-driven lung adenocarcinomas. *Cancer Discov* **3**, 444–457.

[20] Eke I, Deuse Y, Hehlgans S, Gurtner K, Krause M, Baumann M, Shevchenko A, Sandfort V, and Cordes N (2012). beta(1)Integrin/FAK/cortactin signaling is essential for human head and neck cancer resistance to radiotherapy. *J Clin Invest* **122**, 1529–1540.

[21] Chen L, Gibbons DL, Goswami S, Cortez MA, Ahn YH, Byers LA, Zhang X, Yi X, Dwyer D, and Lin W, et al (2014). Metastasis is regulated via microRNA-200/ZEB1 axis control of tumour cell PD-L1 expression and intratumoral immunosuppression. *Nat Commun* **5**, 5241.

[22] Li CW, Xia W, Huo L, Lim SO, Wu Y, Hsu JL, Chao CH, Yamaguchi H, Yang NK, and Ding Q, et al (2012). Epithelial-mesenchymal transition induced by TNF-alpha requires NF-kappaB-mediated transcriptional upregulation of Twist1. *Cancer Res* **72**, 1290–1300.

[23] Li XY, Zhou X, Rowe RG, Hu Y, Schlaepfer DD, Ilic D, Dressler G, Park A, Guan JL, and Weiss SJ (2011). Snail1 controls epithelial-mesenchymal lineage commitment in focal adhesion kinase-null embryonic cells. *J Cell Biol* **195**, 729–738.

[24] Luo SW, Zhang C, Zhang B, Kim CH, Qiu YZ, Du QS, Mei L, and Xiong WC (2009). Regulation of heterochromatin remodelling and myogenin expression during muscle differentiation by FAK interaction with MBD2. *EMBO J* **28**, 2568–2582.

[25] Serrels A, Lund T, Serrels B, Byron A, McPherson RC, von Kriegsheim A, Gomez-Cuadrado L, Canel M, Muir M, and Ring JE, et al (2015). Nuclear FAK Controls Chemokine Transcription, Tregs, and Evasion of Anti-tumor Immunity. *Cell* **163**, 160–173.

[26] Flotho A and Melchior F (2013). Sumoylation: a regulatory protein modification in health and disease. *Annu Rev Biochem* **82**, 357–385.

[27] Bettermann K, Benesch M, Weis S, and Haybaeck J (2012). SUMOylation in carcinogenesis. *Cancer Lett* **316**, 113–125.

[28] Gazdar AF, Girard L, Lockwood WW, Lam WL, and Minna JD (2010). Lung cancer cell lines as tools for biomedical discovery and research. *J Natl Cancer Inst* **102**, 1310–1321.

[29] Ramirez RD, Sheridan S, Girard L, Sato M, Kim Y, Pollack J, Peyton M, Zou Y, Kurie JM, and Dimaio JM, et al (2004). Immortalization of human bronchial epithelial cells in the absence of viral oncoproteins. *Cancer Res* **64**, 9027–9034.

[30] Zhang Y, Gong Y, Hu D, Zhu P, Wang N, Zhang Q, Wang M, Aldeewan A, Xia H, and Qu X, et al (2015). Nuclear SIPA1 activates integrin beta1 promoter and promotes invasion of breast cancer cells. *Oncogene* **34**, 1451–1462.

[31] Gil del Alcazar CR, Hardebeck MC, Mukherjee B, Tomimatsu N, Gao X, Yan J, Xie XJ, Bachoo R, Li L, and Habib AA, et al (2014). Inhibition of DNA double-strand break repair by the dual PI3K/mTOR inhibitor NVP-BEZ235 as a strategy for radiosensitization of glioblastoma. *Clin Cancer Res* **20**, 1235–1248.

[32] Konstantinidou G, Bey EA, Rabellino A, Schuster K, Maira MS, Gazdar AF, Amici A, Boothman DA, and Scaglioni PP (2009). Dual phosphoinositide 3-kinase/mammalian target of rapamycin blockade is an effective radiosensitizing strategy for the treatment of non-small cell lung cancer harboring K-RAS mutations. *Cancer Res* **69**, 7644–7652.

[33] Chen YJ, Shie MY, Hung CJ, Wu BC, Liu SL, Huang TH, and Kao CT (2014). Activation of focal adhesion kinase induces extracellular signal-regulated kinase-mediated osteogenesis in tensile force-subjected periodontal ligament fibroblasts but not in osteoblasts. *J Bone Miner Metab* **32**, 671–682.

[34] Gibbons DL, Lin W, Creighton CJ, Zheng S, Berel D, Yang Y, Raso MG, Liu DD, Wistuba II, and Lozano G, et al (2009). Expression signatures of metastatic capacity in a genetic mouse model of lung adenocarcinoma. *PLoS One* **4**, e5401.

[35] Zheng S, El-Naggar AK, Kim ES, Kurie JM, and Lozano G (2007). A genetic mouse model for metastatic lung cancer with gender differences in survival. *Oncogene* **26**, 6896–6904.

[36] Yang Y, Ahn YH, Chen Y, Tan X, Guo L, Gibbons DL, Ungewiss C, Peng DH, Liu X, and Lin SH, et al (2014). ZEB1 sensitizes lung adenocarcinoma to metastasis suppression by PI3K antagonism. *J Clin Invest* **124**, 2696–2708.

[37] Yang Y, Ahn YH, Gibbons DL, Zang Y, Lin W, Thilaganathan N, Alvarez CA, Moreira DC, Creighton CJ, and Gregory PA, et al (2011). The Notch ligand Jagged2 promotes lung adenocarcinoma metastasis through a miR-200-dependent pathway in mice. *J Clin Invest* **121**, 1373–1385.

[38] Chan KT, Bennin DA, and Huttenlocher A (2010). Regulation of adhesion dynamics by calpain-mediated proteolysis of focal adhesion kinase (FAK). *J Biol Chem* **285**, 11418–11426.

[39] Chen Q, Xu R, Zeng C, Lu Q, Huang D, Shi C, Zhang W, Deng L, Yan R, and Rao H, et al (2014). Down-regulation of Gli transcription factor leads to the inhibition of migration and invasion of ovarian cancer cells via integrin beta4-mediated FAK signaling. *PLoS One* **9**, e88386.

[40] Ward KK, Tancioni I, Lawson C, Miller NL, Jean C, Chen XL, Uryu S, Kim J, Tarin D, and Stupack DG, et al (2013). Inhibition of focal adhesion kinase (FAK) activity prevents anchorage-independent ovarian carcinoma cell growth and tumor progression. *Clin Exp Metastasis* **30**, 579–594.

[41] Camacho CV, Mukherjee B, McEllin B, Ding LH, Hu B, Habib AA, Xie XJ, Nirodi CS, Saha D, and Story MD, et al (2010). Loss of p15/Ink4b accompanies tumorigenesis triggered by complex DNA double-strand breaks. *Carcinogenesis* **31**, 1889–1896.

[42] Cho JH, Robinson JP, Arave RA, Burnett WJ, Kircher DA, Chen G, Davies MA, Grossmann AH, VanBrocklin MW, and McMahon M, et al (2015). AKT1 Activation Promotes Development of Melanoma Metastases. *Cell Rep* **13**, 898–905.

[43] Guan X (2015). Cancer metastases: challenges and opportunities. *Acta Pharm Sin B* **5**, 402–418.

[44] Albasri A, Fadhil W, Scholefield JH, Durrant LG, and Ilyas M (2014). Nuclear expression of phosphorylated focal adhesion kinase is associated with poor prognosis in human colorectal cancer. *Anticancer Res* **34**, 3969–3974.

[45] Lim ST, Miller NL, Chen XL, Tancioni I, Walsh CT, Lawson C, Uryu S, Weis SM, Cheresh DA, and Schlaepfer DD (2012). Nuclear-localized focal adhesion kinase regulates inflammatory VCAM-1 expression. *J Cell Biol* **197**, 907–919.

[46] Lim ST, Chen XL, Lim Y, Hanson DA, Vo TT, Howerton K, Larocque N, Fisher SJ, Schlaepfer DD, and Ilic D (2008). Nuclear FAK promotes cell proliferation and survival through FERM-enhanced p53 degradation. *Mol Cell* **29**, 9–22.

[47] Kadare G, Toutant M, Formstecher E, Corvol JC, Carnaud M, Boutterin MC, and Girault JA (2003). PIAS1-mediated sumoylation of focal adhesion kinase activates its autophosphorylation. *J Biol Chem* **278**, 47434–47440.

[48] Schaller MD, Hildebrand JD, Shannon JD, Fox JW, Vines RR, and Parsons JT (1994). Autophosphorylation of the focal adhesion kinase, pp125FAK, directs SH2-dependent binding of pp60src. *Mol Cell Biol* **14**, 1680–1688.

[49] Fincham VJ and Frame MC (1998). The catalytic activity of Src is dispensable for translocation to focal adhesions but controls the turnover of these structures during cell motility. *EMBO J* **17**, 81–92.

[50] Netherton SJ and Bonni S (2010). Suppression of TGFbeta-induced epithelial-mesenchymal transition like phenotype by a PIAS1 regulated sumoylation pathway in NMuMG epithelial cells. *PLoS One* **5**, e13971.

[51] Lim ST, Mikolon D, Stupack DG, and Schlaepfer DD (2008). FERM control of FAK function: implications for cancer therapy. *Cell Cycle* **7**, 2306–2314.